Introduction to Congenital Heart Disease Anatomy

4

Pierangelo Renella and J. Paul Finn

4.1 Introduction

Imaging of the complex anatomy associated with many forms of congenital heart disease (CHD) requires knowledge of the morphology of the various cardiac chambers, valves, and extra-cardiac vasculature. For the cardiac diagnostician, assembling together the pieces of disordered anatomy is best done with the so-called segmental approach. This approach breaks down the cardiovascular anatomy sequentially, considering first the position of the abdominal viscera, next the cardiac atria, then the looping pattern of the ventricles, and, finally, the position of the semilunar valves and anatomic orientation of the great arteries. In this manner, the various forms of CHD may be precisely identified and the proper management applied by the clinician. The large field of view, good spatial and temporal resolution cine imaging, coupled with three-dimensional multiplanar reconstruction and volume rendering capability of angiographic images, as well as the lack of ionizing radiation exposure, make cardiac magnetic resonance (CMR) the ideal imaging modality for the initial evaluation and serial follow-up of patients with CHD. This holds particularly true for adult and postoperative patients who may have suboptimal echocardiographic imaging windows. This chapter introduces the segmental approach to the diagnosis of CHD vis-à-vis CMR imaging. Each "segment" of the cardiovascular system is described with particular attention paid to the distinguishing features of normal structures so that abnormal features may be more clearly identified. Salient examples of pathology in each segment are also presented with their relevant clinical features.

4.2 Viscero-Atrial Anatomy and Morphology

The specific arrangement of the various thoracoabdominal organs is commonly described as the viscero-atrial "situs." Situs may be classified as *solitus* (normal arrangement), *inversus*, or *ambiguous* (Fig. 4.1) [2, 3]. In viscero-atrial situs solitus, the abdominal and thoracic organs are arranged in the normal fashion, with the liver on the right side, and the spleen and stomach on the left. In addition, the right-sided lung is normally trilobed with an eparterial bronchus, while the left-sided lung has two lobes and a hyparterial bronchus. In viscero-atrial situs solitus, the morphologically left atrium is left-sided and posterior to the morphologically right atrium. Conversely, the morphologically right atrium resides rightward and anterior to the morphologically left atrium.

Supplementary Information The online version contains supplementary material available at https://doi.org/10.1007/978-3-031-29235-4_4.

P. Renella (✉)
Department of Radiology Sciences, David Geffen School of Medicine, Ronald Reagan UCLA Medical Center, Los Angeles, CA, USA

Department of Pediatric Cardiology, UC-Irvine College of Medicine, Children's Hospital Orange County, Orange, CA, USA

University of California Los Angeles (UCLA), Los Angeles, CA, USA

Division of Pediatric Cardiology, CHOC Children's Hospital, Orange, CA, USA
e-mail: prenella@mednet.ucla.edu

J. P. Finn
Department of Radiology Sciences, David Geffen School of Medicine, Ronald Reagan UCLA Medical Center, Los Angeles, CA, USA

University of California Los Angeles (UCLA), Los Angeles, CA, USA

Department of Radiology, Diagnostic Cardiovascular Imaging Section, UCLA, Los Angeles, CA, USA
e-mail: pfinn@mednet.ucla.edu

M. A. Syed, R. H. Mohiaddin (eds.), *Magnetic Resonance Imaging of Congenital Heart Disease*,
https://doi.org/10.1007/978-3-031-29235-4_4

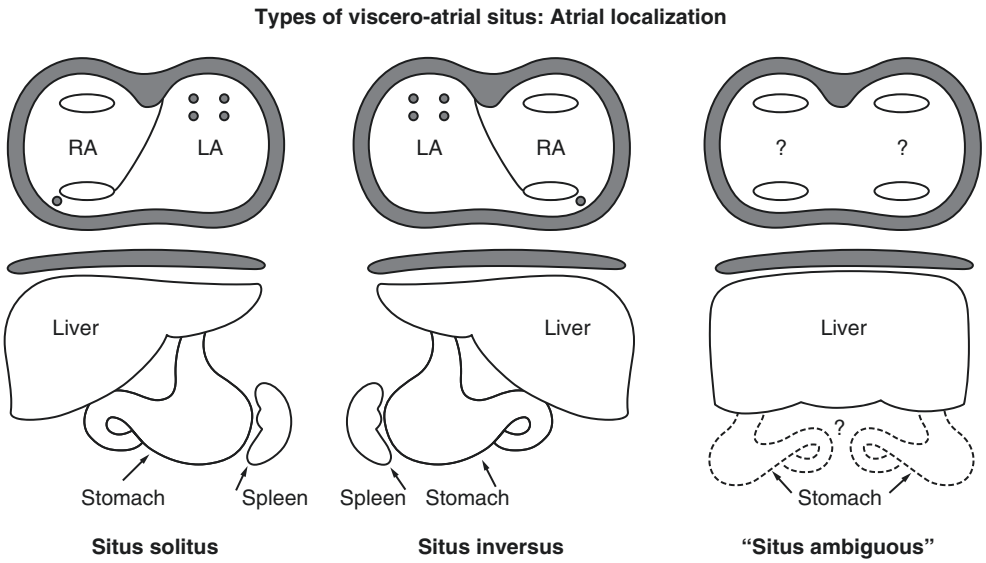

Fig. 4.1 Types of viscero-atrial situs [1]. Shown are the three types of spatial arrangement of the visceral organs and the cardiac atria. Situs *solitus* is the normal configuration with the stomach and spleen on the left side of the body and the liver on the right. Situs *inversus* is the mirror image of situs solitus. The term situs *ambiguous* is applied when there is ambiguity with respect to the specific sidedness of the organs, and the atrial morphology cannot be precisely determined. *RA* right atrium, *LA* left atrium

Table 4.1 Morphological features of the right and left atria

Left atrium	Right atrium
Thin "finger-like" appendage	Broad pyramidal shaped appendage
Smooth wall	Pectinate muscles
Pulmonary venous connections	Crista terminalis
Ostium secundum	Coronary sinus ostium
	Connection of the inferior vena cava
	Connection of the superior vena cava

Morphological features of left and right atria are presented in Table 4.1. Situs "inversus" refers to the mirror image of the normal arrangement. The third category, in which elements of both situs solitus and inversus coexist in the same patient, is termed situs ambiguous (Fig. 4.1). Several different permutations of the thoracic and abdominal organ locations are possible in situs ambiguous, including the presence of two morphologically left or right atria and/or two morphologically left or right bronchi. The liver may be either on the left side or transverse in location. The stomach may be found on either side of the abdominal cavity [3, 4].

4.2.1 Heterotaxy Syndrome

In the heterotaxy syndrome, various aberrations of thoracoabdominal organ right-left orientation may be seen (Fig. 4.2). There exist several published definitions of heterotaxy. A unified definition was proposed by the International Nomenclature Committee for Pediatric and Congenital Heart Disease Nomenclature Working Group [3]. According to this definition, heterotaxy is "… an abnormality where the internal thoraco-abdominal organs demonstrate abnormal arrangement across the left-right axis of the body." This definition excludes patients with pure situs inversus and includes patients with situs ambiguous. Heterotaxy may be associated with either the absence of a spleen (asplenia) or with multiple spleens (polysplenia). Asplenia has also been labeled "bilateral right-sidedness," and polysplenia has been referred to as "bilateral left-sidedness." For example, a patient with heterotaxy and asplenia (i.e., bilateral right-sidedness) may have bilateral morphologically right-sided bronchi and atria, while in heterotaxy with polysplenia, there may be bilateral morphologically left-sided bronchi and atria. Considerable anatomic variation can exist among patients with asplenia or polysplenia.

Heterotaxy syndrome is uncommon, occurring in only approximately 1% of patients with congenital heart disease (CHD) [5]. However, when present, it is often associated with severe cardiac abnormalities (Table 4.2). The 1-year survival without surgical intervention is poor (<15% in asplenia and <50% in polysplenia) [6, 7]. In spite of specialized palliative medical and surgical strategies, approximately one-third of patients will die or require orthotopic heart transplantation within 35 years of Fontan surgery [8].

Transthoracic echocardiography and cardiac catheterization have long been successfully applied in patients with heterotaxy syndrome. CMR has been also shown to be of value in this patient population and, in fact, may be superior in terms of precise localization of the thoracoabdominal organs, bronchial anatomy, cardiac chamber morphology, and connections of the pulmonary and systemic veins often encountered in these patients [9, 10].

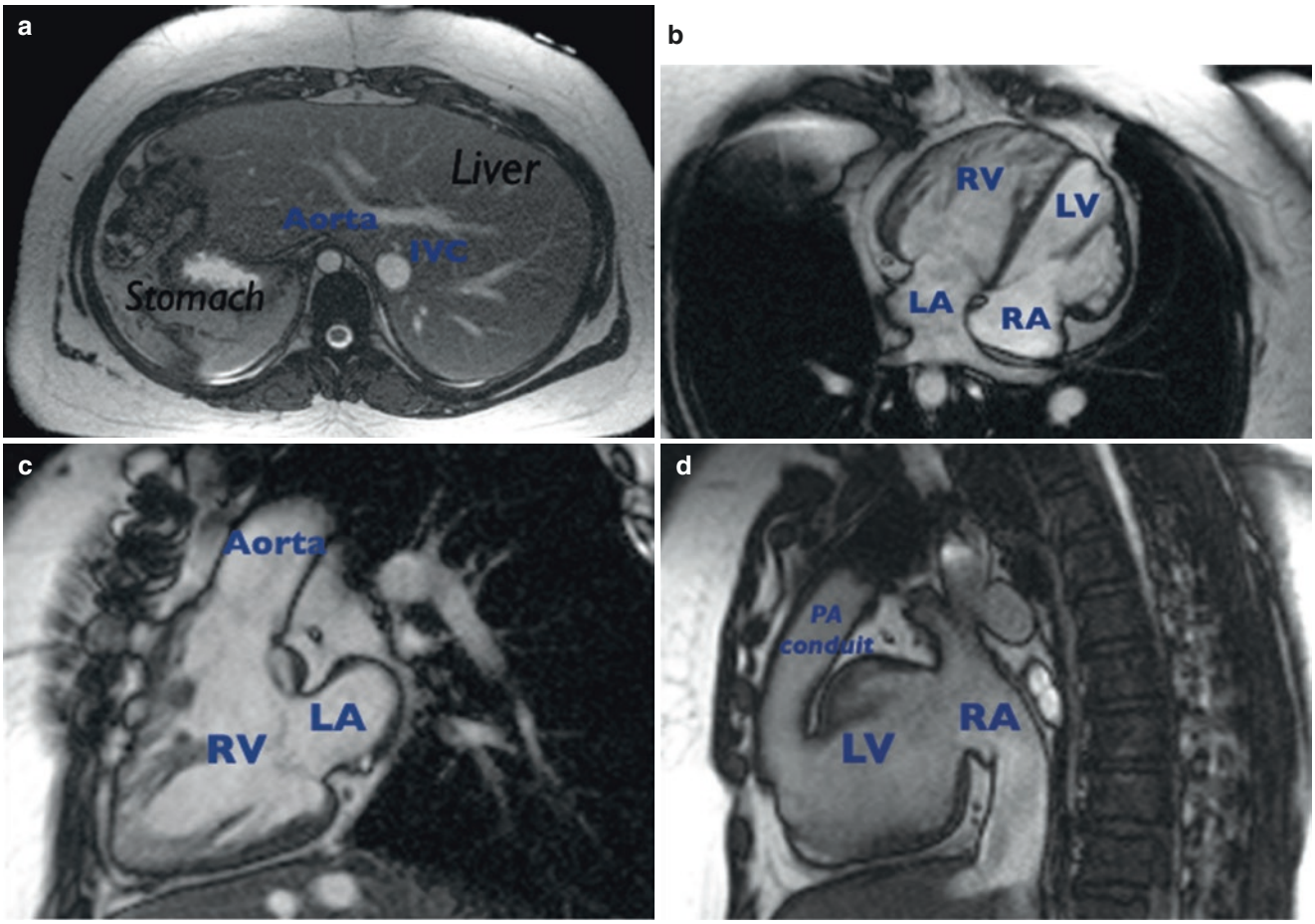

Fig. 4.2 Heterotaxy syndrome with viscero-atrial situs inversus (MR steady-state free precession imaging). (**a**) SSFP image in the axial plane through abdomen demonstrating visceral situs *inversus* (left-sided liver and right-sided stomach). Note also that the IVC is on the left and the aorta is on the right. (**b**) SSFP image of atrioventricular discordance in a patient with l-loop transposition of the great arteries. In this patient, there is viscero-atrial situs inversus with discordant connections of the atrial to their respective ventricles. (**c**) Same patient as in (**b**) depicting abnormal atrioventricular and ventriculo-arterial discordance ("double discordance"). The RV connects to the anteriorly and leftward positioned (l-malposed) aorta. (**d**) Same patient as in (**b**). This patient has undergone surgical LV to PA conduit placement to bypass native subpulmonary stenosis. *IVC* inferior vena cava, *LV* left ventricle, *RV* right ventricle, *LA* left atrium, *RA* right atrium, *PA* pulmonary artery

Table 4.2 Cardiac malformations associated with heterotaxy syndrome

Anatomic feature	Asplenia ("bilateral right-sidedness")	Polysplenia ("bilateral left-sidedness")
Liver position	Transverse (76–91%)	Transverse (50–67%)
Lung lobes	Bilaterally trilobed (81–93%)	Bilaterally bilobed (72–88%)
Bronchial morphology	Bilaterally eparterial (95%)	Bilaterally hyparterial (68–88%)
Superior vena cava	Bilateral (46–71%)	Bilateral (33–50%)
Inferior vena cava	Interrupted with azygos continuation (rare)	Interrupted with azygos continuation (58–100%)
Pulmonary veins	Total anomalous connection (64–72%)	Anomalous drainage (normal connection) due to atrial septal malalignment (37–50%)
Atrial morphology	Common atrium (57%)	Common atrium (25–30%)
Cardiac crux	AV canal defects (84–92%)	AV canal defects (80%)
Ventricles	Functional single ventricle (44–55%)	Functional single ventricle (37%)
Cardiac position	Dextrocardia (36–41%)	Dextrocardia (33–42%)
Ventriculo-arterial connection	Double outlet right ventricle (82%); transposition of the great arteries (9%)	Double outlet right ventricle (17–37%)

Adapted from Bartram et al. [5]

4.3 Veno-Atrial Connections

Two distinct venous systems connect to the cardiac atria: the *systemic* veins (inferior vena cava, superior vena cava, hepatic veins, coronary sinus) and the *pulmonary* veins (Fig. 4.3). The systemic veins carry deoxygenated blood to the morphologically right atrium. Conversely, the pulmonary veins carry oxygenated blood to the morphologically left atrium. In fact, as already reviewed in Table 4.1, the very connections of the coronary sinus (CS) and inferior vena cava (IVC) to the right atrium help define it as the morphologically right atrium (Table 4.1). Similarly, the connections of the pulmonary veins are one of the distinguishing features of a morphologically left atrium.

4.3.1 Systemic Venous Connections

The superior vena cava (SVC) forms from both brachiocephalic (innominate) veins. There is usually a single right SVC, although it is possible to have a single left SVC (with an absent right SVC) or bilateral SVCs (with or without a bridging vein). The right SVC normally courses anterior to the right pulmonary artery and against the posterolateral aspect of the ascending aorta before connects to the roof of the morphologically right atrium (Fig. 4.3a) [11].

The IVC receives systemic venous drainage from the lower body, including the retroperitoneum, portal circulation, and lower extremities (Fig. 4.3b). After traversing superiorly, it courses within the liver and through the diaphragmatic hiatus to reach the floor of the right atrium [11]. This normally occurs on the right side of the body but may be on the left or even midline, depending on the atrial situs. In atrial situs inversus, for example, the IVC may connect to a morphologically right atrium located on the left side of midline. The intrahepatic portion of the IVC may be absent (interrupted) as a normal variant or in the heterotaxy syndrome, particularly the polysplenia subtype (as described above). In this case, the IVC blood would continue to the SVC via the more posteriorly located azygos vein [12, 13].

The coronary sinus (CS) is the confluence of the majority of the coronary venous drainage and opens normally to the morphologically right atrium (Fig. 4.3c). It may also receive a persistent left superior vena cava (LSVC) or an anomalously connected pulmonary vein (or veins). In rare instances, the CS may be "unroofed" and thus open directly into the morphologically left atrium, resulting in an abnormal right-to-left shunt. Complete atresia of the CS ostium has also been reported [11].

The hepatic veins typically drain to the IVC directly and/or the floor of the morphologically right atrium (Fig. 4.3d). In the case of an interrupted IVC with azygos continuation, the hepatic veins will connect directly to the floor of the morphologically right atrium. Naturally, when there is viscero-atrial situs inversus, the hepatic veins may be found left of midline. In situs ambiguous, the hepatic veins may drain in the midline to a common atrium of indeterminate morphology or have separate connections to one or both atria.

4.3.1.1 Total Anomalous Systemic Venous Connection

Very rarely all the systemic veins connect anomalously to the morphologically left atrium. This is known as total anomalous systemic venous connection. In this lesion, there is usually a single left SVC connecting to an unroofed CS, such that venous drainage from the upper body drains directly to the left atrium. In addition, the IVC is interrupted with continuation via the azygos vein to the left SVC. Finally, the hepatic veins also anomalously connect to the floor of the left atrium. Most often, this condition occurs in the setting of heterotaxy and complex cyanotic CHD [12]. In isolation, this defect would be expected to cause profound cyanosis. However, arterial saturation may be somewhat improved by a bidirectional atrial level shunt (e.g., in the setting of a common atrium). An example of a variant of this lesion is depicted in Fig. 4.4. Surgical repair may consist of an intra-atrial baffle constructed to direct the IVC, SVC, and CS flow appropriately to the right atrium [12].

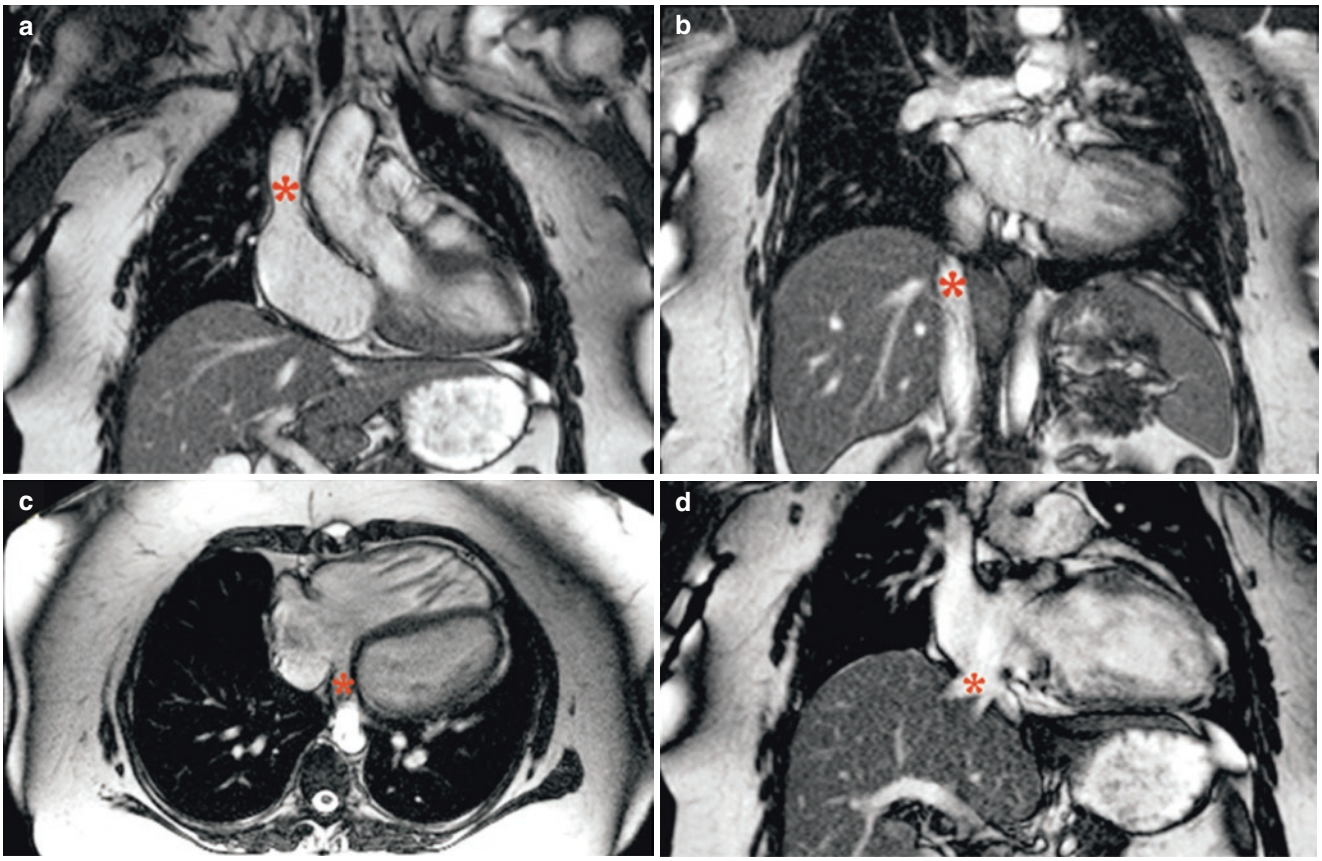

Fig. 4.3 Normal systemic and pulmonary veno-atrial connections. (**a**) The superior vena cava (*SVC*) carries venous drainage from the upper body to the morphologically right atrium (*asterisk*). (**b**) The inferior vena cava (*IVC*) carries lower body venous drainage to the morphologically right atrium (*RA*), and indeed, this IVC connection is one of the defining features of an RA (*asterisk*). (**c**) The coronary sinus (*CS*) ostium is another defining feature of a morphologically RA. It carries the coronary venous blood (*asterisk*). (**d**) The hepatic veins either connect to the IVC and/or directly to the floor of the RA (*asterisk*)

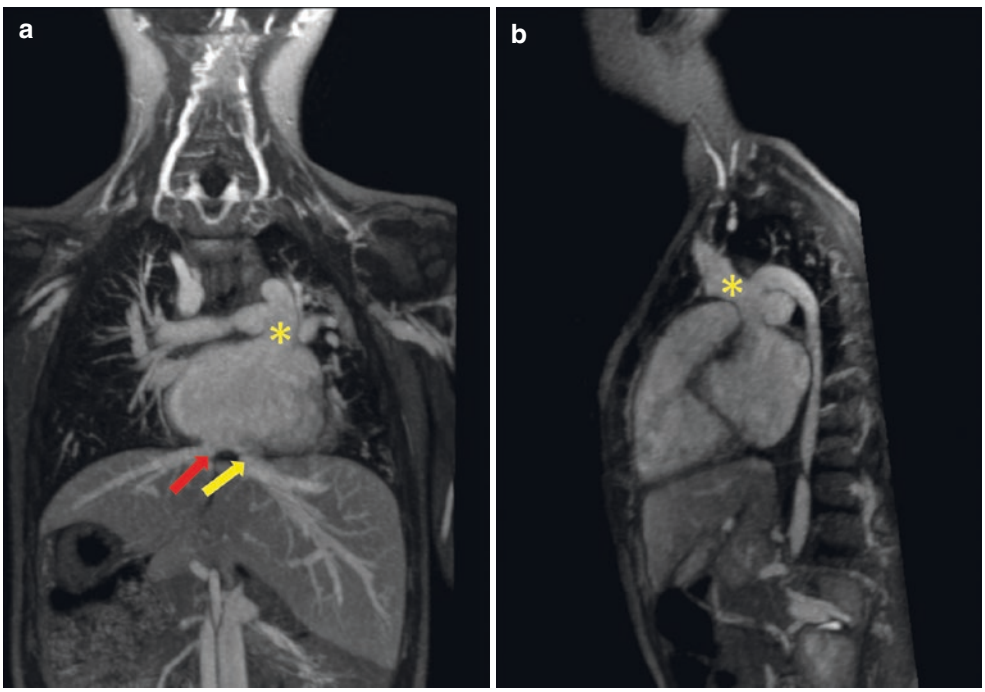

Fig. 4.4 Total anomalous systemic venous connection. Contrast-enhanced MRA maximum intensity projections in the coronal and sagittal planes. (**a**, **b**) Left superior vena cava receiving a dilated azygos vein (due to interruption of the inferior vena cava) with direct connection to the left-sided atrium (yellow asterisks). The right hepatic vein connects to the left-sided atrium (yellow arrow). In this patient, the only systemic vein not to connect to the left-sided atrium is the right hepatic vein (red arrow). Its connection is to the right-sided atrium

4.3.2 Pulmonary Venous Connections

In the normal heart, venous drainage from the lungs returns via the pulmonary veins to the morphologically left atrium. In the normal configuration, two pulmonary veins (one upper and one lower) from each lung course to the morphologically left atrium. The right upper and lower pulmonary veins course posteriorly to the right atrium and SVC, while the left upper and lower pulmonary veins course just anterior to the descending thoracic aorta. The right upper pulmonary vein is usually formed by branches from the right upper and right middle lobes of the lung. The right upper and right middle pulmonary veins typically join together prior to connecting to the left atrium. However, as a normal variant, the right middle branch may enter the left atrium separately. In addition, it is not uncommon for the two left-sided pulmonary veins to join the atrium as a single common vein [11]. Of clinical interest, the cardiac end of each pulmonary vein contains myocardial cells rather than smooth muscle cells [11]. This area of the pulmonary veins has been implicated in abnormal electrical circuits predisposing patients to atrial fibrillation. As such, the proximal pulmonary veins are potential targets of transcatheter radiofrequency ablation therapy for atrial fibrillation [14]. Pre-procedural planning for treatment of atrial fibrillation via transcatheter ablation often includes CMR imaging [15].

During embryological development of the pulmonary veins, there exist connections between the primitive pulmonary and splanchnic venous plexi. If the common pulmonary vein fails to connect to the posterior morphologically left atrium, these pulmonary and splanchnic connections persist, resulting in anomalous pulmonary venous connections of various types [16]. In the case of total anomalous pulmonary venous connection (TAPVC), all the pulmonary veins retain their embryonic connections to the systemic venous system and do not connect directly to the morphologically left atrium. These connections may become obstructed and present either at birth, or within the first part of infancy, with cyanosis and rapid clinical deterioration. In fact, "obstructed" TAPVC is one of the few surgical emergencies in pediatric cardiology. In partial anomalous pulmonary venous connection (PAPVC), at least one, but not all, of the pulmonary veins connect abnormally.

Three general categories of TAPVC are described based on which systemic veins the anomalous pulmonary veins maintain an embryonic connection to Fig. 4.5. In decreasing order of frequency, these are (1) supracardiac, (2) cardiac, and (3) infradiaphragmatic. When the pulmonary venous connections consist of some combination of these categories, the designation of "mixed" TAPVC is given. The "mixed" form of TAPVC is the least common, occurring in only 8% of patients [18]. "Supracardiac" TAPVC occurs in approximately 50% of the cases and consists of pulmonary venous blood being redirected via a "vertical vein" (to usually the innominate vein) on its way to the right SVC or to a left SVC directly [16]. The "cardiac" form of the disease typically involves drainage of the pulmonary veins directly to the coronary sinus. The "infradiaphragmatic" form of TAPVC is described in detail below.

4.3.2.1 Infradiaphragmatic Total Anomalous Pulmonary Venous Connection (TAPVC)

Although a relatively uncommon form of TAPVC, when the connection of the pulmonary venous confluence to the systemic circulation is via an infradiaphragmatic route, the risk of obstruction and subsequent early clinical deterioration is relatively high. In infradiaphragmatic TAPVC, the pulmonary venous blood courses via a "vertical vein" running parallel to the aorta, through the diaphragm (at the esophageal hiatus), connects to the portal venous system, and then into the hepatic circulation (via the ductus venosus), on its way to the right atrium (Fig. 4.6). This roundabout pathway back to the heart creates multilevel resistance to blood flow. In particular, the more common sites of obstruction are at the level of the vertical vein as it passes through the diaphragm, from closure of the ductus venosus, and/or due to high resistance intrahepatic connections [16]. Additionally, due to the complete mixing of pulmonary and systemic venous blood in the right atrium, patients may be profoundly cyanotic.

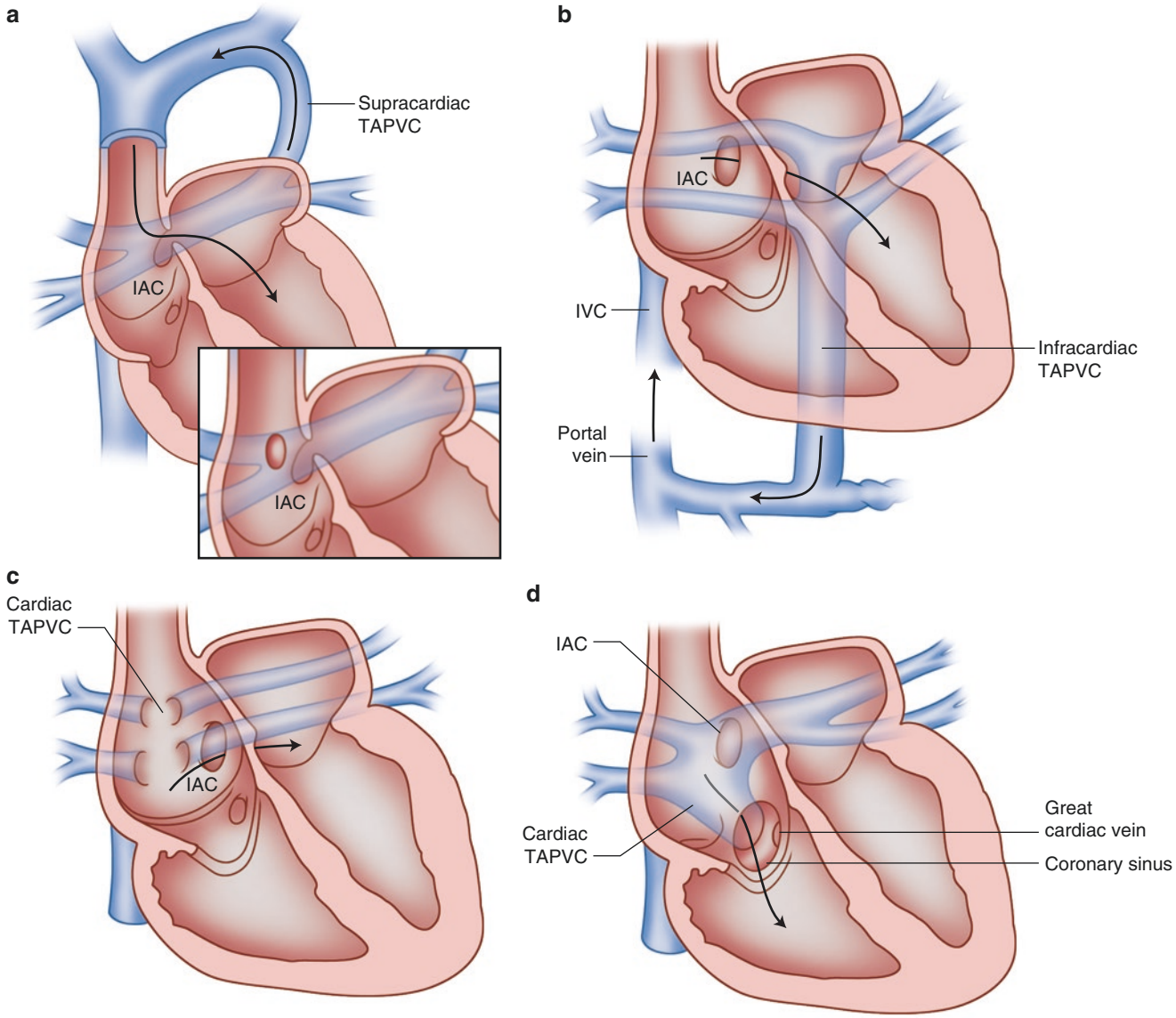

Fig. 4.5 Total anomalous pulmonary venous connection (TAPVC) [17]. This diagram depicts the three general categories of TAPVC. (**a**) Supracardiac TAPVC: the pulmonary venous blood returns to the heart via a vertical vein to the innominate vein and ultimately to the SVC and right atrium. (**b**) Infracardiac (infradiaphragmatic) TAPVC: a particularly insidious subtype of TAPVC due to its relatively higher propensity for pulmonary venous obstruction and clinical deterioration in the neonatal period. (**c**) Cardiac TAPVC shown with direct anomalous pulmonary venous connections to the right atrium (**d**) and with the more common scenario involving anomalous drainage to the right atrium via direct connection of the pulmonary vein confluence with the coronary sinus. *IAC* interatrial communication, *TAPVC* total anomalous pulmonary venous connection. (Copyright 1985 by the Texas Heart Institute, Houston. Illustration by Bill Andrews)

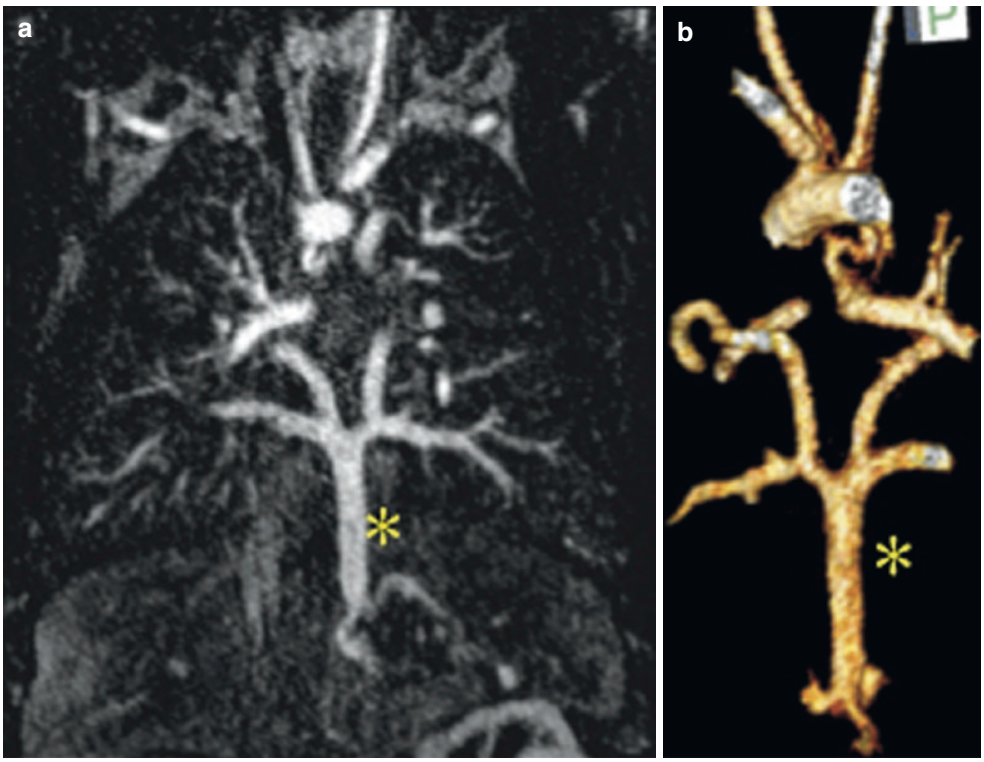

Fig. 4.6 (**a**, **b**) Infradiaphragmatic TAPVC. Infant boy with infradiaphragmatic TAVPC. The *left* panel (**a**) is a coronal projection of a high-resolution contrast-enhanced MR angiogram showing all four pulmonary veins joining a confluence and coursing caudally through the diaphragm via a vertical vein (*asterisk*) toward the liver. It then drains into the portal circulation and subsequently to the IVC. The panel on the *right* (**b**) is a posterior projection of a volume rendered image of the MR angiogram

4.4 Atrioventricular Connections and Ventricular Morphology

The accurate diagnosis of complex CHD depends on correctly identifying the morphology of the heart chambers, the atrioventricular connections, and their specific locations within the chest cavity. The anatomic components that identify the right and left atria are reviewed above (Table 4.1). Like the atria, the left and right ventricles also each have distinguishing morphological features (Table 4.3). Notably, the shape of the morphologically left ventricle (LV) resembles a prolate ellipsoid or "bullet" shape (Fig. 4.7a). It has a smooth basal septal surface (*asterisk*), and the mitral valve apparatus attaches to the free wall rather than the ventricular septum ("septophobic" attachments). The shape of the morphologically right ventricle (RV) is a complex pyramidal shape [19, 20]. It has three distinct parts: (1) inflow portion, (2) body and apex, and an (3) outflow or "infundibulum." There is a moderator band located toward the apex, and the tricuspid valve apparatus attaches to both the ventricular septum ("septophillic" attachments) and the RV free wall (Fig. 4.7b–d).

After establishing the morphology of the atria and ventricles, attention can then be directed to how the chambers connect. In the normal configuration, a given ventricle typically receives inflow of blood only from its respective atrium via one of the two atrioventricular (AV) valves, the mitral or tricuspid valve. Normally, the left atrium connects to the LV via the mitral valve, and the right atrium connects to the RV via the tricuspid valve.

Table 4.3 Morphological features of the ventricles

Left ventricle	Right ventricle
Smooth basal septal surface	Muscular infundibulum (outflow tract)
Fine trabeculations	Coarse trabeculations
Guarded by mitral valve	Guarded by tricuspid valve
Prolate ellipsoid ("bullet") shape	Complex pyramidal shape
	Moderator band
	Relatively thin free wall

Aberrations of these connections are the basis of some forms of CHD. For example, in double inlet left ventricle (DILV), both atrioventricular valves connect to a single morphologically left ventricle (see below). The LV would then give off either the aorta or the pulmonary artery. In these cases, there also exists a small outflow chamber that receives blood from the single left ventricle via a bulboventricular foramen that then connects to the other great artery. This outflow chamber does not have a direct atrioventricular connection (see below) and thus is not labeled a true ventricle in the strict sense.

In the very rare case of a double inlet right ventricle (DIRV), the opposite applies. That is, the single morphologically RV receives the inflow of both the left ("mitral") and

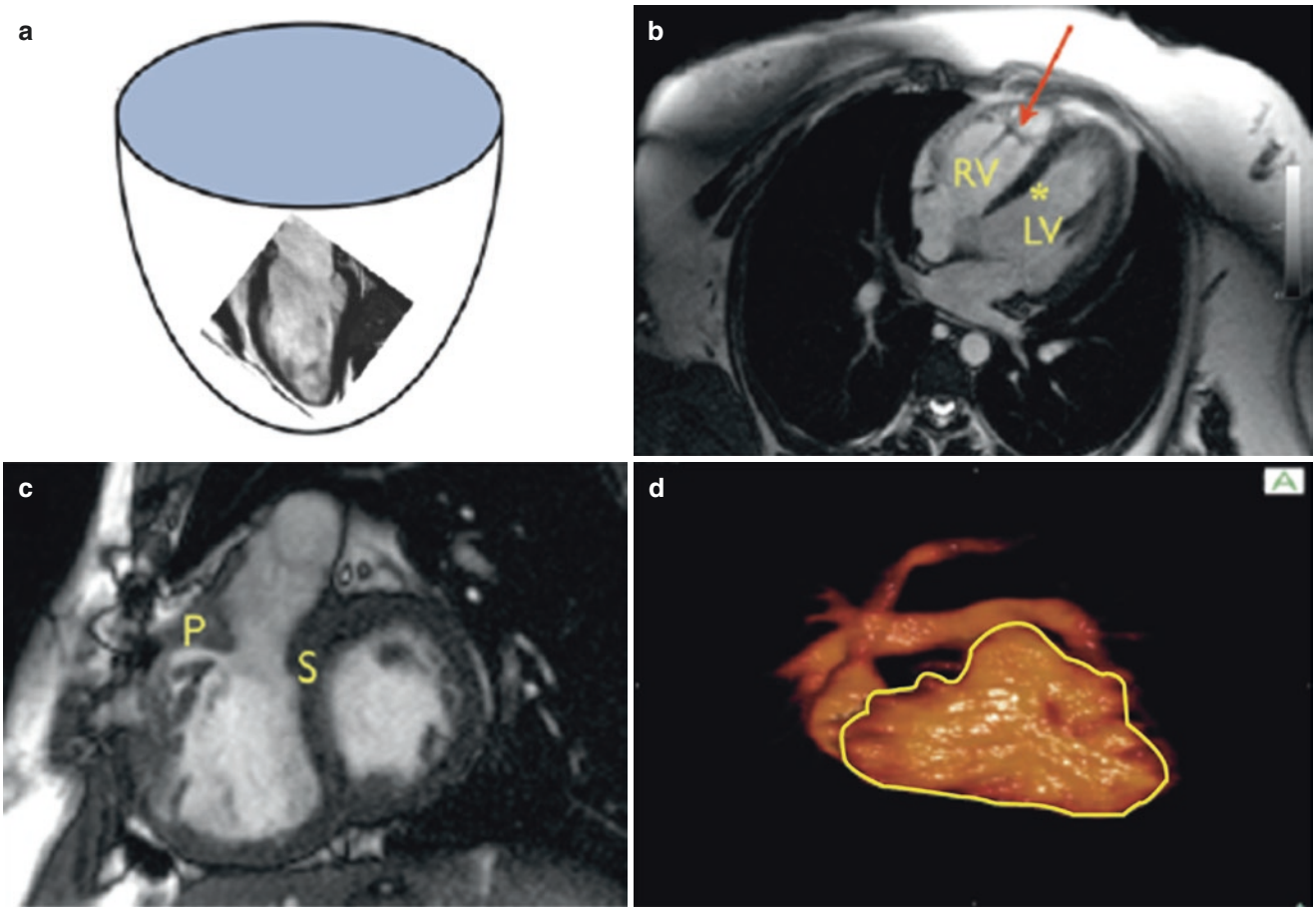

Fig. 4.7 Normal left and right ventricular morphology. (**a**, **b**) The shape of the morphologically left ventricle most closely approximates the shape of a prolate ellipsoid ("bullet" shape). Other distinguishing features include a smooth basal septal surface (*asterisk*) and attachments of the mitral valve to the free wall rather than to the ventricular septum. (**b**) The shape of the morphologically right ventricle is a complex pyramidal shape with an inflow portion, a body and apex, and an outflow portion (infundibulum). The presence of the moderator band (*arrow*) is a very reliable feature of a morphologically right ventricle. (**c**) Other distinguishing features include coarse trabeculations of the ventricular wall, septal band (*S*), parietal band (*P*), and attachments of the tricuspid valve to the ventricular septum as well as the free wall ("septophillic" attachments). (**d**) "Cast" of the right ventricle from a 3D volume rendered high resolution cardiac MR angiogram highlighting the complex geometry typical of an RV (yellow outline)

right ("tricuspid") AV valves and connects to one of the great arteries. Just as in the case of DILV, in DIRV, there also exists a diminutive outflow chamber that connects to the other great artery. DILV and DIRV have also been referred to as types of "univentricular atrioventricular connections."

Conversely, in the case of complete atrioventricular canal defect (AVCD), there are two distinct ventricles with one common AV valve rather than separate mitral and tricuspid valves (see below). When the common AV valve directs blood equally to the two ventricles, it is referred to as a "balanced" AVCD. This results in both ventricles being of adequate size. In "unbalanced" AVCD, however, the common AV valve orifice is directed preferentially toward one of the ventricles, causing the other to become hypoplastic and often not able to handle a full cardiac output. Thus, many patients with unbalanced AVCD are not be candidates for standard surgical closure of the defect and may in fact require "single ventricle" surgical palliation [21].

4.4.1 Unbalanced Right-Dominant Complete Atrioventricular Canal Defect (AVCD)

As described above, the complete form of the atrioventricular canal defect (AVCD), also known as "atrioventricular canal" or "atrioventricular septal defect," is due to incomplete differentiation of the crux of the heart. This creates a primum atrial septal defect (ASD), an inlet ventricular septal defect (VSD), and failure of formation of the right and left halves of the atrioventricular canal which become the mitral and tricuspid valves

[22]. Physiologically, this can result in a large left-to-right shunt and congestive heart failure. AVCD commonly occurs as part of more complex CHD, extracardiac defects, and genetic syndromes. For example, approximately one-half of AVCD patients have Down syndrome [23, 24]. AVCD may also be combined with conotruncal defects (such as tetralogy of Fallot) in some patients, particularly in those with Down syndrome [24, 25]. In general, there are four basic types of AVCD: (1) complete, (2) intermediate, (3) transitional, and (4) partial (Fig. 4.8) [26]. In the complete form, the AV valve has one large common orifice and five or six rudimentary leaflets, along with significant primum ASD and inlet VSD components. In the intermediate form, there remain significant ASD and VSD components, but the AV valve has midline tissue dividing it into two distinct orifices. The transitional form is similar to the intermediate form, except that the VSD component is made smaller by dense attachments of the AV valve leaflets to the crest of the ventricular septum. The partial AVCD is characterized by simply a primum ASD and a cleft mitral valve, but no VSD. The tricuspid valve is usually normal. Note that all forms of AVCD, except the complete form, feature a "cleft" in the mitral valve that points toward the interventricular septum. In addition, based on the alignment of the common AV valve with the ventricles, the flow of blood may be directed either equally to the two ventricles ("balanced" AVCD) or may favor one ventricle over the other ("unbalanced" AVCD). Unbalanced AVCD can be either right- or left-dominant, depending on which ventricle is larger (Fig. 4.9). A "balanced" complete AVCD is presented in Movie 4.1.

4.4.2 Double Inlet Left Ventricle (DILV)

Double inlet left ventricle (DILV) is the most common form of "single ventricle" and occurs due to the persistence of the primitive state of the bulboventricular loop and failure of the atria to properly align themselves with the AV valves [27]. This results in the morphologically left ventricle receiving the inflow of both atria. In the majority of cases, the outflow of the left ventricle usually occurs via a transposed pulmonary artery, and the aorta arises from a rudimentary outflow chamber positioned anterior and leftward of the left ventricle (Fig. 4.10) [28]. Blood from the LV reaches the great artery arising from the outflow chamber via a bulboventricular foramen. This outflow pathway is prone to obstruction in the sub-valvar, valvar, and supra-valvar areas, as well as distally along length of the vessel. For example, in cases where the aorta arises from the diminutive outflow chamber, there is an

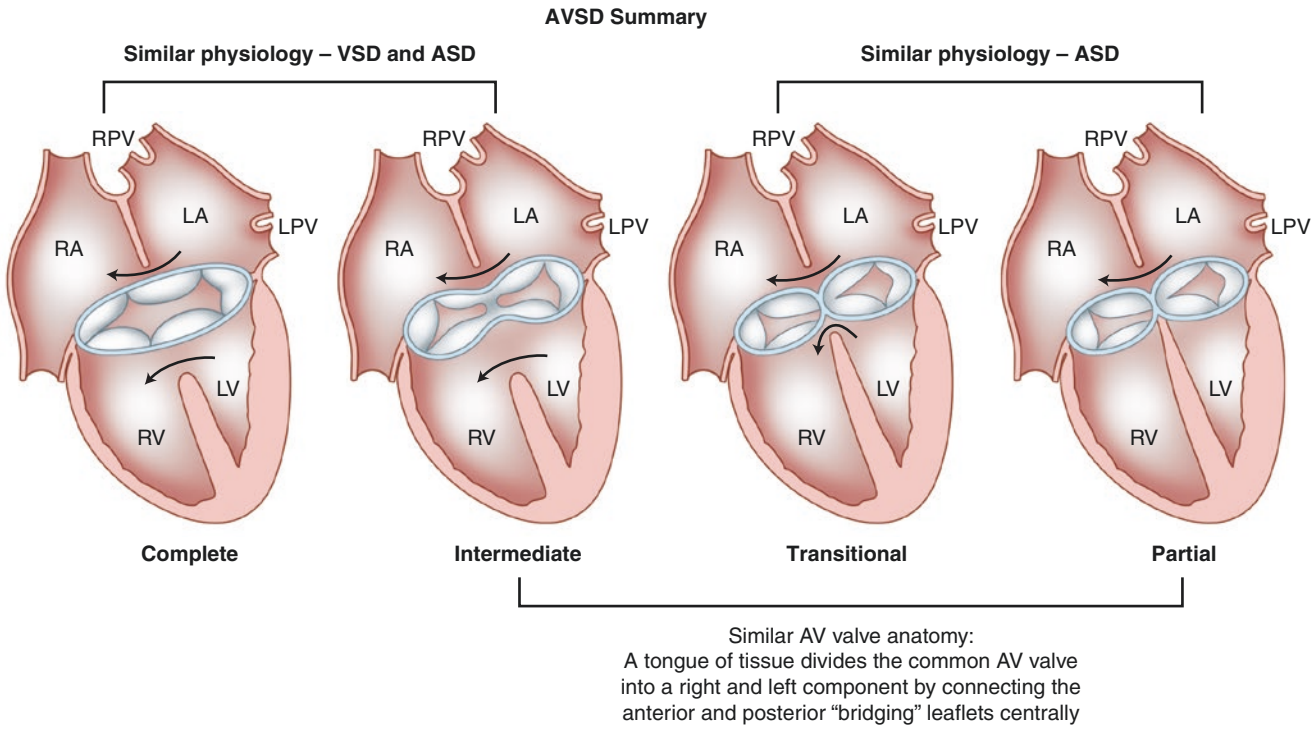

Fig. 4.8 Summary of atrioventricular canal defects (AVCD) [26]. The four basic types of atrioventricular canal defects (AVCD). The "complete" AVCD features large primum ASD and inlet VSD components with a truly single common AV valve orifice. The "intermediate" form is similar to the complete form, but the AV valves have separate orifices, even though there remains a "cleft" in the mitral valve. The "transitional" AVCD is similar to the intermediate form, but the AV valves have separate orifices, there is a mitral valve cleft, and there is a relatively smaller VSD component. In the "partial" form of AVCD, there is no VSD component, the tricuspid valve is normal, and the mitral valve is cleft. *ASD* atrial septal defect, *VSD* ventricular septal defect, *AV* atrioventricular

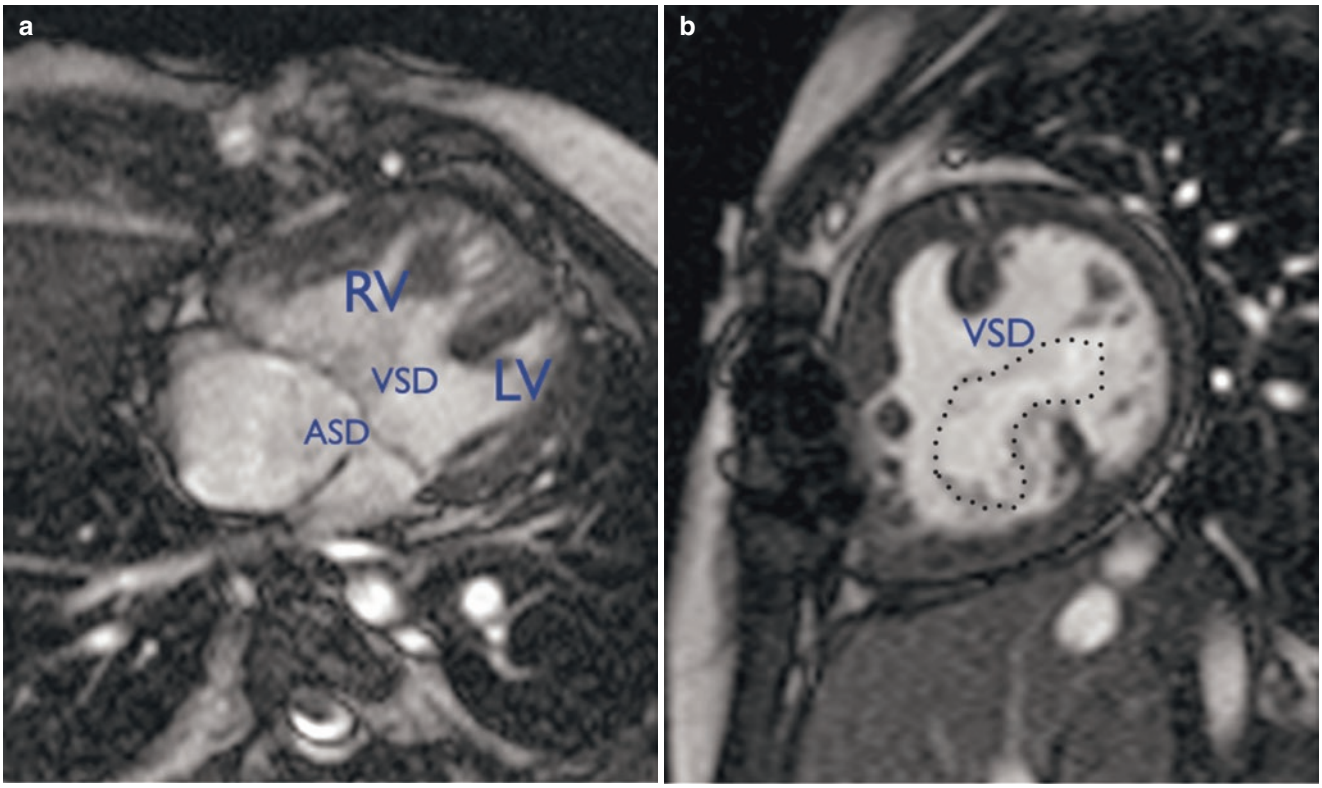

Fig. 4.9 Unbalanced right-dominant AVCD. (**a**) SSFP MR imaging in the horizontal long axis ("four chamber") view of a right-dominant AVCD. Clearly shown is the primum ASD, the large inlet VSD, and the common AV valve which spans across the cardiac crux and separates the ASD superiorly and the VSD inferiorly. Note the size discrepancy between the ventricles with the RV being dominant. (**b**) SSFP MR imaging in the short axis plane. The common AV valve is disproportionately aligned with the RV, thus resulting in LV hypoplasia. *SSFP* steady-state free precession, *ASD* atrial septal defect, *VSD* ventricular septal defect, *AV* atrioventricular, *RV* right ventricle, *LV* left ventricle

increased risk of associated coarctation. In approximately 15% of cases, the great arteries are oriented normally, the so-called Holmes heart, with the aorta arising from the LV and the pulmonary artery from the outflow chamber. It is also possible to encounter a double inlet right ventricle (DIRV), but this lesion is considerably rarer.

Physiologically, all types of "functionally single ventricle" exhibit total mixing of venous and arterial blood at the atrial and/or ventricular levels. Depending on the balance of pulmonary versus systemic blood flow, the patient may be deeply cyanotic, less cyanotic but in congestive heart failure from a large left-to-right shunt, or have relatively well-balanced systemic and pulmonary circulations with mild cyanosis but not in congestive heart failure.

Management of patients with single ventricle anatomy consists of a staged surgical strategy with the goal of separating the systemic venous circulation from the heart. First, the superior vena cava is anastomosed directly to the branch pulmonary arteries. Later, this strategy culminates in the Fontan surgery where the inferior vena cava is also redirected to the branch pulmonary arteries using an artificial conduit (see Fig. 4.11 and Movie 4.2).

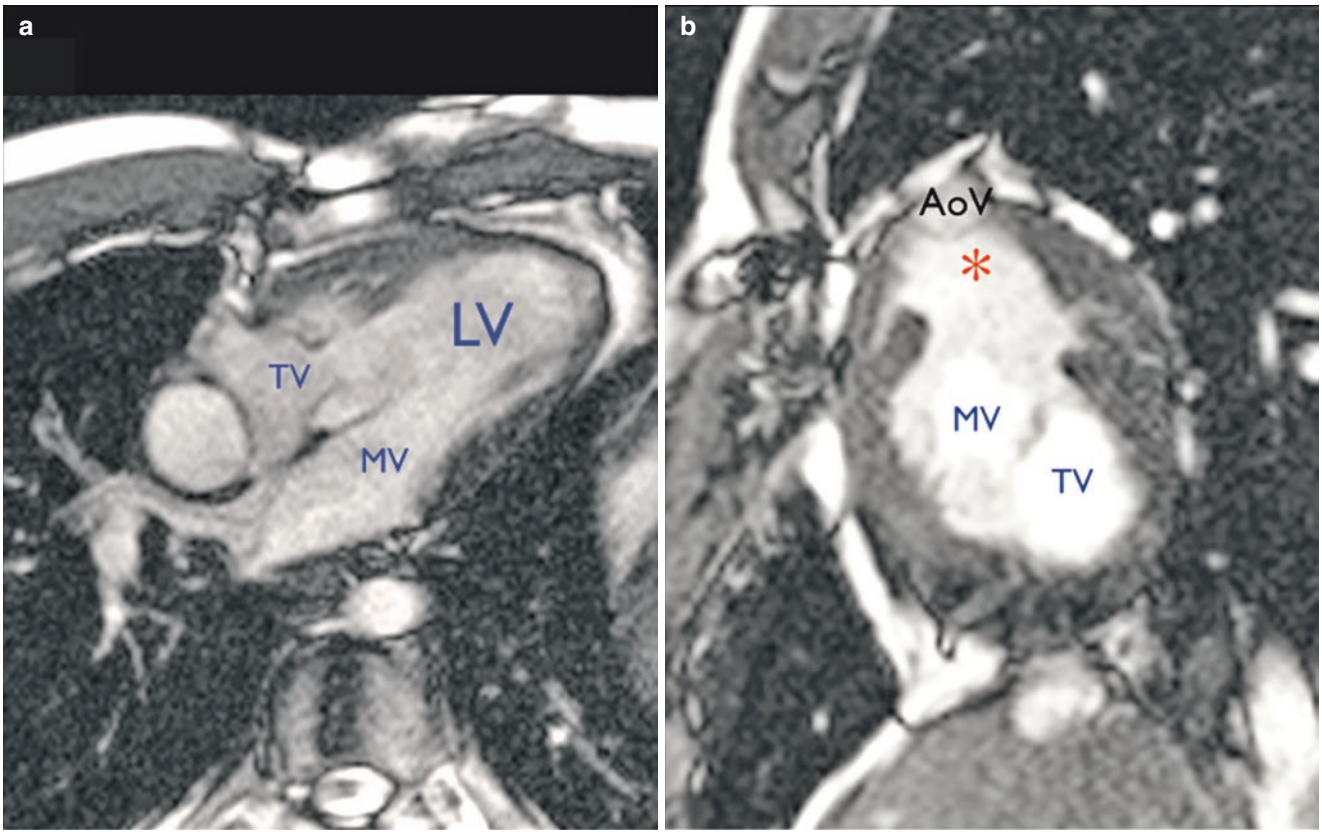

Fig. 4.10 Double inlet left ventricle (DILV) [28]. (**a**) SSFP MR imaging in the horizontal long axis ("four chamber") view of a patient with DILV. Both the left AV or "mitral" (*MV*) and right AV or "tricuspid" valves (*TV*) are aligned with the single left ventricle (*LV*). (**b**) SSFP MR imaging in the short axis plane. Note that both atrioventricular valves are clearly aligned with the left ventricle (LV). The aortic valve (*AoV*) arises from the anterior and leftward diminutive "outflow chamber" (*asterisk*), as there is no true right ventricle in this lesion. *AV atrioventricular*

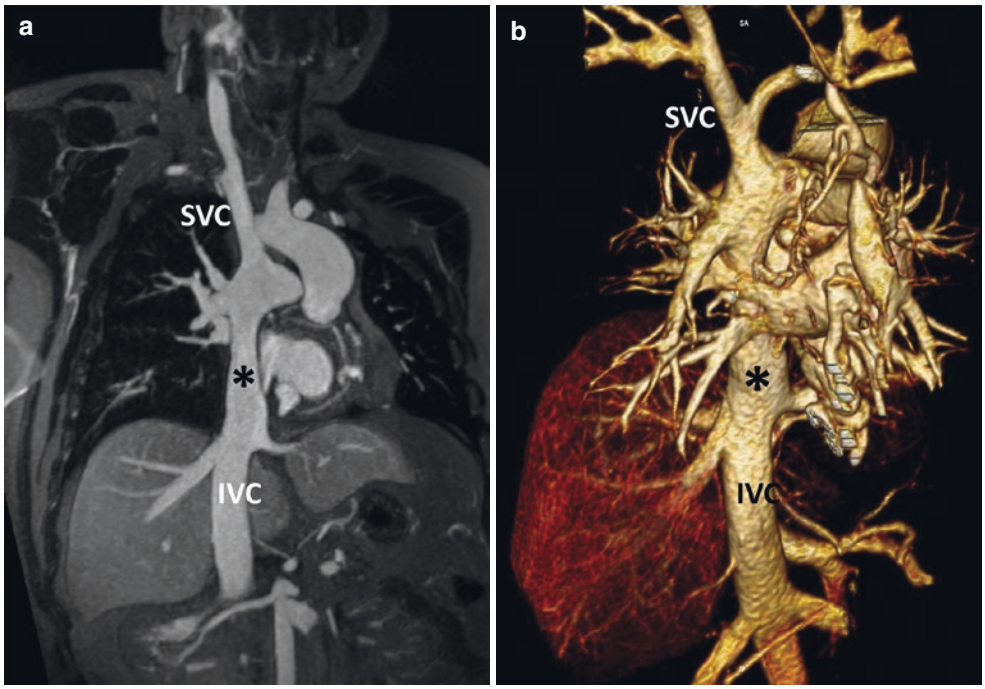

Fig. 4.11 Fontan circulation in two adult patients with single ventricle anatomy who have undergone surgical Fontan completion. (**a**) Ferumoxytol-enhanced MR angiogram 3D multiplanar reconstruction in the coronal plane demonstrating connections of the superior vena cava (SVC) and the inferior vena cava (IVC) to the branch pulmonary arteries. The extracardiac artificial Fontan conduit connecting the IVC to the pulmonary circulation is noted by the black asterisk. The native SVC was directly anastomosed to the branch pulmonary arteries during a prior surgery. (**b**) Posterior projection of a 3D volume rendered ferumoxytol-enhanced MR angiogram in a different patient with situs inversus who required a *left*-sided Fontan connection. The black asterisk again denotes the Fontan conduit

4.5 Ventriculo-Arterial Connections

Embryologically, both the aortic and pulmonary valves become associated with a "pedestal" of tissue known as the conus arteriosus overlying the morphologically RV. According to one prominent theory, beginning at approximately 30–34 days of gestation, the conus under the aortic valve begins to resorb. This allows for the aortic valve to move into its conventional position posterior and rightward of the pulmonary valve. When the subaortic conus persists and the sub-pulmonary conus resorbs instead, the aortic valve position is anterior and rightward of the pulmonary valve and becomes associated with the RV, leaving the pulmonary valve to connect to the LV. If the ventricles are normally looped, this "dextro-transposition" of the aortic valve may lead to a condition known as d-loop or complete transposition of the great arteries (TGA) (see below) [29]. Alternatively, when both sides of the conus fail to resorb, association of both the aortic and pulmonary valves with the RV occurs and is termed "double outlet right ventricle."

4.5.1 D-Loop Transposition of the Great Arteries (D-Loop TGA, Complete TGA)

In d-loop TGA, the aorta is positioned anterior and rightward of the pulmonary artery and is connected to the morphologically RV, while the pulmonary artery arises more posteriorly and leftward from the LV (Fig. 4.12 and Movie 4.3). It is the most commonly encountered type of "discordance" of the ventriculo-arterial connections, occurring in approximately 2.4 in 10,000 live births [30]. D-loop TGA is often found in isolation with no other associated cardiac or extracardiac pathology. The most common subtype is "simple" d-loop TGA. That is, the ventricles are normally looped, and there are no associated ventricular septal defects (VSD) or other cardiac abnormalities. A VSD may be present in approximately one-half of patients and has been termed "complex" d-loop TGA. With a VSD present, there may be associated pulmonary valve stenosis/atresia, sub-valvar pulmonary stenosis, or coarctation of the aorta [31].

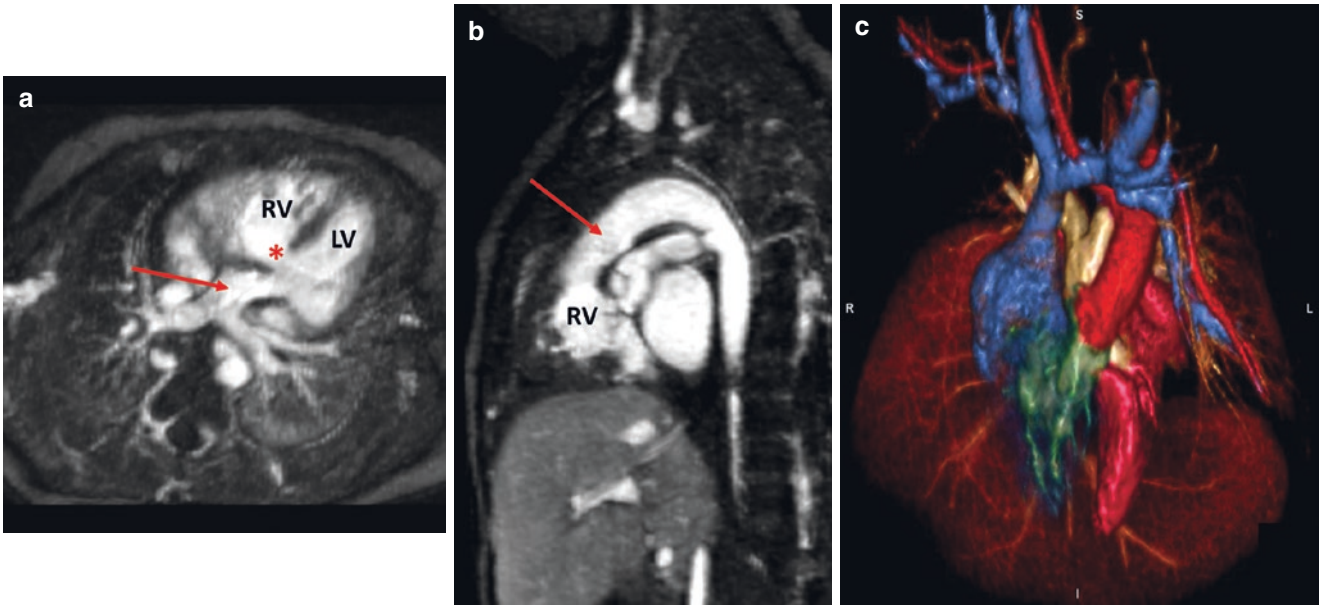

Fig. 4.12 D-loop transposition of the great arteries (d-TGA) in a neonate. Ferumoxytol-enhanced MR angiogram 3D multiplanar reconstruction in the axial and sagittal planes (**a**, **b**). (**a**) The pulmonary artery (red arrow) arises posteriorly from the left ventricle (LV). There is a ventricular septal defect (VSD) present as noted by the red asterisk. (**b**) The aorta (red arrow) arises anteriorly from the right ventricle (RV). (**c**) Anterior projection of a colorized 3D volume rendering in the same patient demonstrating the anterior aorta arising from the RV (both colored in red). The more posterior pulmonary artery is shown colored in gold

Physiologically, deoxygenated blood from the RV is distributed to the systemic circulation via the transposed aorta. Oxygenated blood is sent back to the lungs, resulting in inefficient gas exchange. As a result, profound cyanosis may occur, particularly in the absence of adequate intermixing between the two circulations. Mixing usually occurs via an atrial septal defect, VSD, and/or patent ductus arteriosus. Inadequate mixing will eventually lead to worsening cyanosis and death if not promptly addressed.

4.5.2 L-Loop Transposition of the Great Arteries ("Congenitally Corrected" Transposition)

In contrast to d-loop TGA, the l-loop variety is considerably less common, occurring in approximately 2–7 in 100,000 live births or 0.5% of all CHD [30, 32]. L-loop TGA is characterized by "doubly discordant" atrioventricular and ventriculo-arterial connections. As the name implies the ventricles are l-looped. This allows for the alignment of the morphologically RV with the morphologically left atrium and vice versa for the right atrium and LV. The aortic valve in this condition is most often positioned anterior and leftward of the pulmonary valve and is connected to the right ventricle. As such, patients are not typically cyanotic because oxygenated blood from the left atrium courses to the aorta, albeit via a "systemic" right ventricle. It is for this reason that l-loop TGA has been referred to as "congenitally corrected" or "physiologically corrected" transposition.

The vast majority of l-loop TGA patients have associated cardiac structural abnormalities. These include VSD, left ventricular outflow tract (sub-pulmonary) stenosis, Ebstein's malformation of the tricuspid valve, mitral valve dysplasia, and a 2% per year incidence of spontaneous complete heart block [32]. In addition, dextrocardia or mesocardia may be seen in association with l-loop TGA [33].

4.6 Arterial Malformations (Vascular Rings and Slings)

Certain malformations of the aorta and pulmonary arteries exist that may lead to external tracheal and/or esophageal compression [34]. The most common types are presented in Table 4.4. A complete vascular "ring" occurs when various components of the aortic arch and ligamentum arteriosum completely encircle the trachea and esophagus causing vari-

Table 4.4 Most common vascular malformations causing external tracheal and/or esophageal compression

Left aortic arch with aberrant right subclavian artery (incomplete vascular ring)
Double aortic arch (complete vascular ring)
Right aortic arch with aberrant left subclavian artery (from a diverticulum of Kommerell) and left ligamentum arteriosum (complete vascular ring)
Left pulmonary artery sling

Adapted from Kussman et al. [35]

able degrees of external compression of these structures. With incomplete vascular rings, and in the case of a vascular "sling," tracheal and/or esophageal compression can occur, but the involved vascular components do not completely encircle the trachea and esophagus.

Vascular rings and slings arise from aberrations in the complex sequence of formation and regression of the six pairs of embryonic aortic arches that connect the truncus arteriosus and aortic sac with the paired dorsal aortae. This process has been well described elsewhere [34, 36]. Edwards proposed a simplified model of the various types of vascular rings and slings by way of a conceptual "hypothetical double arch with bilateral ductus arteriosus" model (Fig. 4.13) [37]. The Edwards model may be further simplified into a series of line drawings, as shown in Fig. 4.14 [34]. By imagining the regression of specific segments of this double arch, one may arrive at the various types of existing aortic arch anomalies (Fig. 4.14).

Although aortic arch anomalies consist of less than 1% of all CHD, they may cause varying degrees of tracheal and/or esophageal compression and can be diagnosed early in life. Some cases are not diagnosed until adulthood and others may never be diagnosed at all. In the patient with significant wheezing, stridor, feeding intolerance, and/or recurrent airway obstruction, it is important to maintain a high index of suspicion for vascular malformations, particularly when other more common causes have been ruled out [35].

4.6.1 Complete Vascular Rings

The most common complete vascular ring is the double aortic arch. In this lesion, the two aortic arches persist and surround the trachea and esophagus (Fig. 4.14a). In only 5% of cases are both arches patent, however. In up to 80% of the time the right arch is patent and the left arch is atretic. The left arch is patent and the right arch atretic in the remainder of cases [38]. It is important to remember that atretic arch segments are not usually visualized by imaging techniques

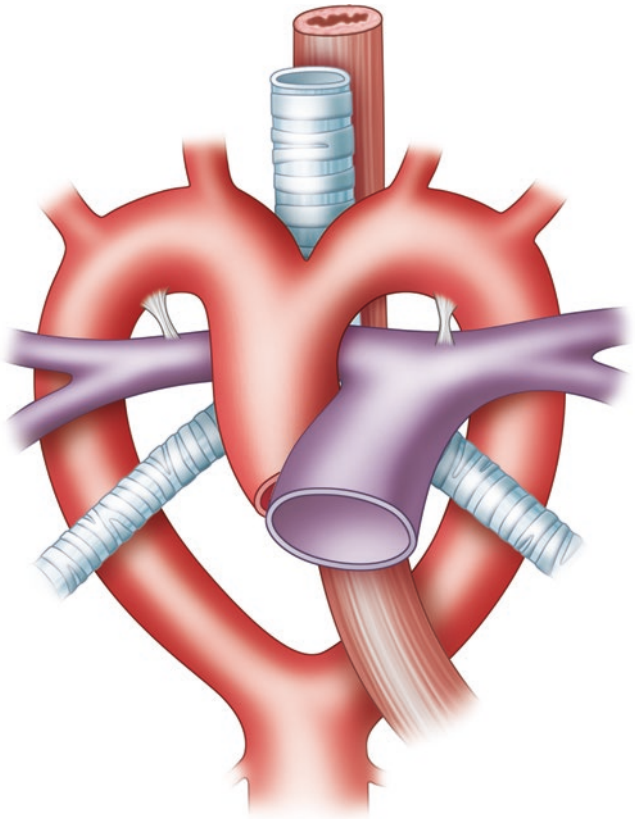

Fig. 4.13 Edwards' hypothetical "double aortic arch with bilateral ductus arteriosus" model [34]

and must be inferred based upon the appearance of vascular outpouchings or based on knowledge of their typical location. This also holds true for the ductus arteriosus portion of vascular rings.

The second most common complete vascular ring is formed by a right aortic arch with aberrant left subclavian artery and a left ductus arteriosus (Fig. 4.14c and Movie 4.4). In this lesion, the ring is formed by the left common carotid artery, the transverse aortic arch, a posterior aberrant left subclavian artery, and the left-sided ductus arteriosus. The left subclavian artery arises from a remnant of the left fourth arch called the diverticulum of Kommerell, which encircles the esophagus posteriorly [38].

4.6.2 Incomplete Vascular Ring

A left aortic arch with an aberrant right subclavian artery is the most common aortic arch variant with an incidence of approximately 0.5% in the general population (Fig. 4.14b)

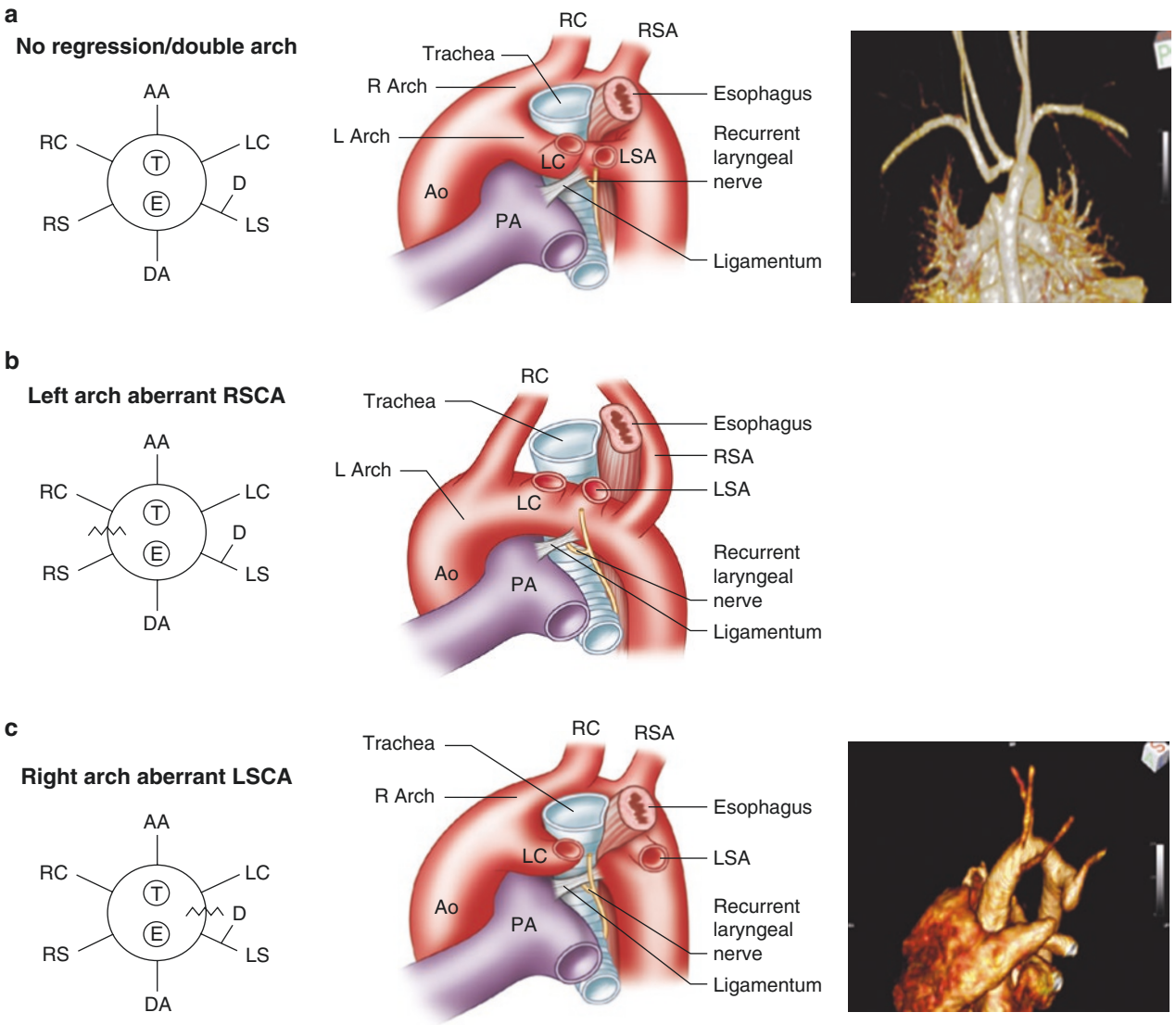

Fig. 4.14 Vascular rings [34, 38]. Line diagram illustrating the origin of various types of vascular rings and slings (derived from Edwards' double arch model shown in Fig. 4.13). (**a**) The double aortic arch is the most common type of vascular ring. In this lesion, neither of the dorsal aortae regresses. The *right most* panel is a 3D volume rendered MR angiogram of a double aortic arch with an atretic left arch. The atretic arch does not fill with contrast, and thus its presence must be inferred. (**b**) Left aortic arch with aberrant right subclavian artery is an incomplete ring and, as such, infrequently causes symptoms. (**c**) Right aortic arch with aberrant left subclavian artery is the second most common type of vascular ring. The *right most* panel is a 3D volume rendered MR angiogram of this lesion

[39]. This variation of aorta anatomy forms an incomplete vascular ring as the aberrant right subclavian compresses the esophagus posteriorly as it traverses toward the right arm. This anatomic variant only rarely has any clinical consequences.

4.6.3 Left Pulmonary Sling

In left pulmonary artery sling, the left branch pulmonary artery arises more distally than normal, branching directly off of the right pulmonary artery. The left pulmonary artery then courses around the right bronchus and then between the trachea and esophagus in order to reach the left lung hilum (Fig. 4.15). Approximately half of patients may have associated complete tracheal rings rather than the normal "C-" shaped tracheal rings. Posterior tracheal compression from the left pulmonary artery in conjunction with tracheal luminal narrowing by the complete tracheal rings often manifests as stridor, wheezing, and recurrent pneumonia in the neonatal period [40].

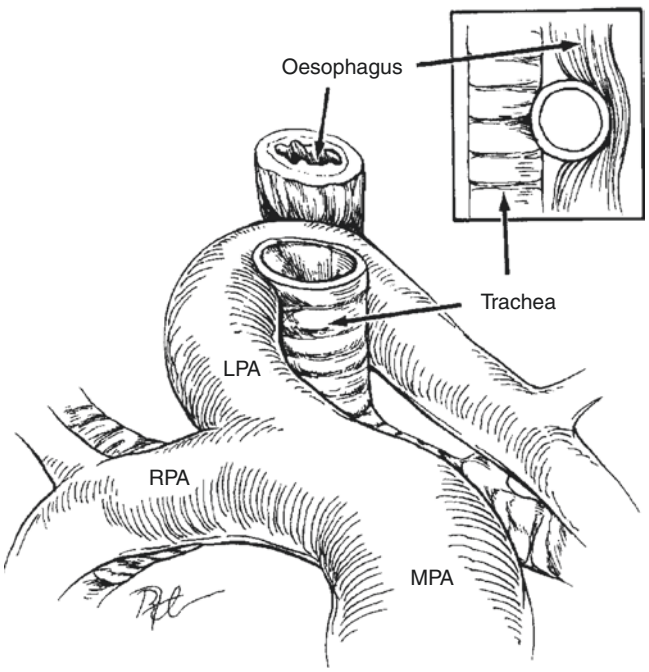

Fig. 4.15 Left pulmonary artery sling [38]. The left pulmonary artery arises more distally off the right pulmonary artery and makes an acute turn, coursing in between the trachea and esophagus to reach the left lung hilum. This causes the classic anterior compression of the esophagus seen on conventional upper GI imaging

4.6.4 Coarctation of the Aorta

Narrowing of the aortic isthmus is termed coarctation of the aorta and occurs in 6–8% of infants born with CHD [41]. Severe coarctation most often presents in the first 1–2 weeks of life. After the patent ductus arteriosus closes, there may be inadequate blood flow to the lower body leading to circulatory shock. The typical location of the narrowing is "juxtaductal," which is the area of the aortic isthmus opposite the insertion of the ductus arteriosus (Fig. 4.16). There is often an associated long-segment narrowing of the transverse aortic arch proximal to the area of coarctation. Other associated defects include bicuspid aortic valve, ventricular septal defects, and mitral valve abnormalities.

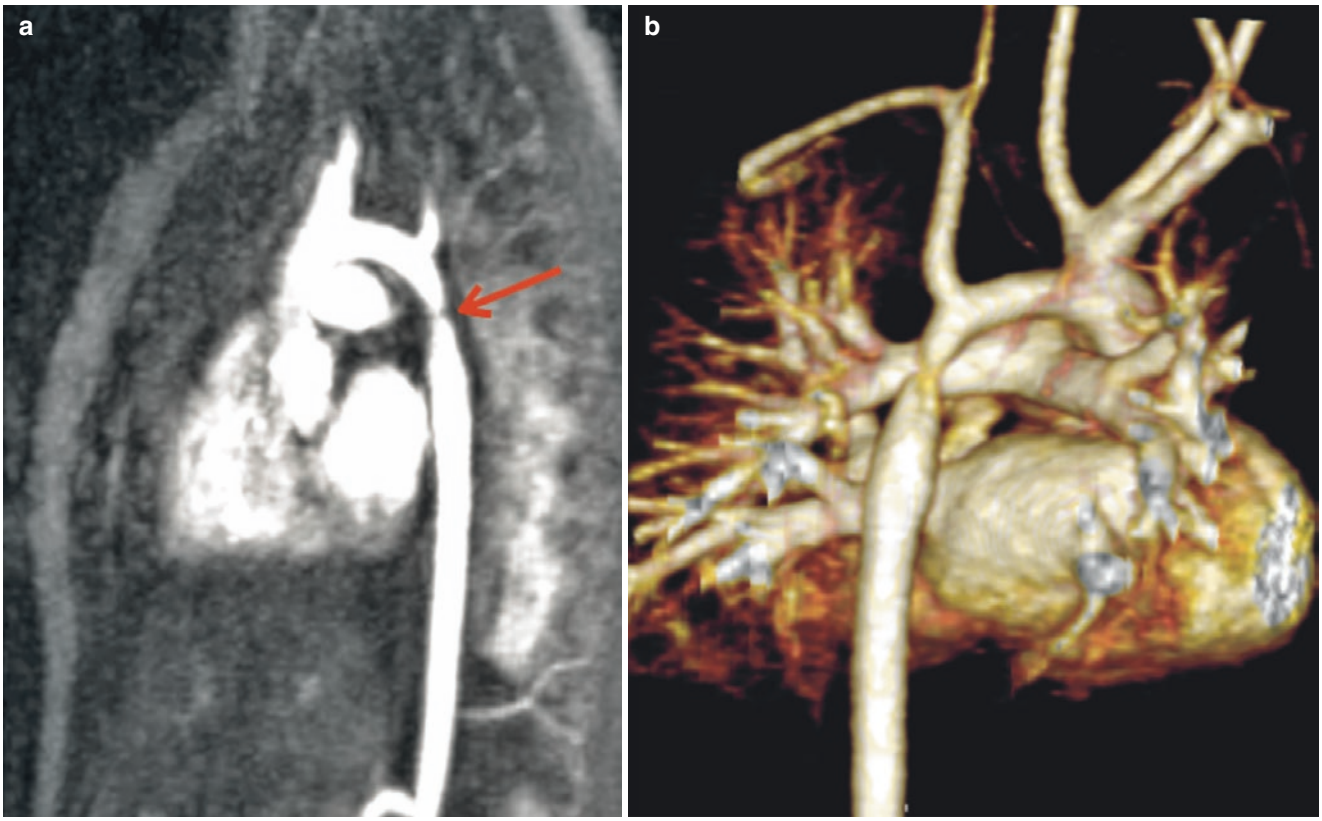

Fig. 4.16 Coarctation of the aorta. (**a**) MR contrast-enhanced angiogram 3D multiplanar reconstruction in the sagittal plane demonstrating a juxtaductal coarctation of the aorta (*red arrow*) in a neonate. (**b**) 3D volume rendered MR contrast-enhanced angiogram of the same

4.7 Conclusion

CMR imaging is ideally suited for the characterization of congenital anatomic and physiologic aberrations of the cardiovascular system. The advantages of CMR over other imaging modalities include its noninvasive nature, absence of ionizing radiation, the use of a non-iodinated contrast agent, comprehensive view of both the intracardiac structures and extra-cardiac vasculature, quantification of blood flow, and myocardial tissue characterization. Continuing technical developments in the areas of image processing speed, increased spatial resolution, and machine learning will ensure CMR's integral role in the comprehensive assessment of patients with congenital heart disease [42, 43].

Practical Pearls

- CMR imaging allows for a comprehensive assessment of intracardiac structures, extra-cardiac vasculature, and blood flow.
- The noninvasive nature of CMR and the lack of ionizing radiation and iodinated contrast make CMR imaging advantageous for congenital heart disease patients who require serial lifelong imaging studies.
- In the initial diagnosis and serial evaluation of congenital heart disease, CMR should be considered complimentary to other traditional imaging techniques such as echocardiography and cardiac catheterization.
- CMR in congenital heart disease is ideally performed and interpreted in concert with specially trained radiologists, cardiologists, and cardiothoracic surgeons.

References

1. Praagh RV, Praagh SV. Morphologic anatomy. In: Keane JF, Flyer DC, Lock J, editors. Nadas' pediatric cardiology. 2nd ed. Philadelphia, PA: Saunders Elsevier; 2006. p. 27–37.
2. Praagh RV. Segmental approach to diagnosis. In: Keane JE, Flyer DC, Lock J, editors. Nadas' pediatric cardiology. 2nd ed. Philadelphia, PA: Saunders Elsevier; 2006. p. 39–46.
3. Jacobs JP, Anderson RH, Weinberg PM, Walters HL III, Tchervenkov CI, Del Duca D, et al. The nomenclature, definition and classification of cardiac structures in the setting of heterotaxy. Cardiol Young. 2007;17(Suppl 2):1–28. https://doi.org/10.1017/S1047951107001138.
4. Cohen MS, Anderson RH, Cohen MI, Atz AM, Fogel M, Gruber PJ, et al. Controversies, genetics, diagnostic assessment, and outcomes relating to the heterotaxy syndrome. Cardiol Young. 2007;17(Suppl 2):29–43. https://doi.org/10.1017/S104795110700114X.
5. Bartram U, Wirbelauer J, Speer CP. Heterotaxy syndrome -- asplenia and polysplenia as indicators of visceral malposition and com-

plex congenital heart disease. Biol Neonate. 2005;88(4):278–90. https://doi.org/10.1159/000087625.
6. Peoples WM, Moller JH, Edwards JE. Polysplenia: a review of 146 cases. Pediatr Cardiol. 1983;4(2):129–37. https://doi.org/10.1007/BF02076338.
7. Van Mierop L, Gessner I, Schiebler GL. Asplenia and polysplenia syndrome. Birth Defects. 1972;8:74–84.
8. Poh CL, Cordina RL, Iyengar AJ, Zannino D, Grigg LE, Wheaton GR, et al. Pre- and post-operative determinants of transplantation-free survival after Fontan. The Australia and New Zealand experience. Int J Cardiol Heart Vasc. 2021;35:100825. https://doi.org/10.1016/j.ijcha.2021.100825.
9. Geva T, Vick GW III, Wendt RE, Rokey R. Role of spin echo and cine magnetic resonance imaging in presurgical planning of heterotaxy syndrome. Comparison with echocardiography and catheterization. Circulation. 1994;90(1):348–56. https://doi.org/10.1161/01.cir.90.1.348.
10. Hong YK, Park YW, Ryu SJ, Won JW, Choi JY, Sul JH, et al. Efficacy of MRI in complicated congenital heart disease with visceral heterotaxy syndrome. J Comput Assist Tomogr. 2000;24(5):671–82. https://doi.org/10.1097/00004728-200009000-00002.
11. Edwards WD. Cardiac anatomy and examination of cardiac specimens. In: Allen HD, Driscoll D, Shaddy RE, Feltes TF, editors. Moss and Adams' heart disease in infants, children, and adolescents. Philadelphia, PA: Lippincott Williams & Wilkins; 2008. p. 2–33.
12. Mazzucco A, Bortolotti U, Stellin G, Gallucci V. Anomalies of the systemic venous return: a review. J Card Surg. 1990;5(2):122–33. https://doi.org/10.1111/j.1540-8191.1990.tb00749.x.
13. Celentano C, Malinger G, Rotmensch S, Gerboni S, Wolman Y, Glezerman M. Prenatal diagnosis of interrupted inferior vena cava as an isolated finding: a benign vascular malformation. Ultrasound Obstet Gynecol. 1999;14(3):215–8. https://doi.org/10.1046/j.1469-0705.1999.14030215.x.
14. Pappone C, Rosanio S, Oreto G, Tocchi M, Gugliotta F, Vicedomini G, et al. Circumferential radiofrequency ablation of pulmonary vein ostia: a new anatomic approach for curing atrial fibrillation. Circulation. 2000;102(21):2619–28. https://doi.org/10.1161/01.cir.102.21.2619.
15. Beinart R, Nazarian S. Role of magnetic resonance imaging in atrial fibrillation ablation. Curr Treat Opt Cardiovasc Med. 2014;16(6):316. https://doi.org/10.1007/s11936-014-0316-3.
16. Stein P. Total anomalous pulmonary venous connection. AORN J. 2007;85(3):509–20. https://doi.org/10.1016/S0001-2092(07)60123-9; quiz 21–4.
17. Reardon MJ, Cooley DA, Kubrusly L, Ott DA, Johnson W, Kay GL, et al. Total anomalous pulmonary venous return: report of 201 patients treated surgically. Tex Heart Inst J. 1985;12(2):131–41.
18. Keane JF, Fyler DC. Total anomalous pulmonary venous return. In: Keane JF, Lock JE, Flyer DC, editors. Nadas' pediatric cardiology. 2nd ed. Philadelphia, PA: Saunders Elsevier; 2006. p. 773–81.
19. Dorosz JL, Bolson EL, Waiss MS, Sheehan FH. Three-dimensional visual guidance improves the accuracy of calculating right ventricular volume with two-dimensional echocardiography. J Am Soc Echocardiogr. 2003;16(6):675–81. https://doi.org/10.1016/s0894-7317(03)00226-8.
20. Kuhl HP, Schreckenberg M, Rulands D, Katoh M, Schafer W, Schummers G, et al. High-resolution transthoracic real-time three-dimensional echocardiography: quantitation of cardiac volumes and function using semi-automatic border detection and comparison with cardiac magnetic resonance imaging. J Am Coll Cardiol. 2004;43(11):2083–90. https://doi.org/10.1016/j.jacc.2004.01.037.
21. Owens GE, Gomez-Fifer C, Gelehrter S, Owens ST. Outcomes for patients with unbalanced atrioventricular septal defects. Pediatr Cardiol. 2009;30(4):431–5. https://doi.org/10.1007/s00246-008-9376-z.
22. Rogers HM, Edwards JE. Incomplete division of the atrioventricular canal with patent inter-atrial foramen primum, persistent common atrioventricular ostium; report of five cases and review of the literature. Am Heart J. 1948;36(1):28–54. https://doi.org/10.1016/0002-8703(48)90545-6.
23. Dunlop KA, Mulholland HC, Casey FA, Craig B, Gladstone DJ. A ten year review of atrioventricular septal defects. Cardiol Young. 2004;14(1):15–23. https://doi.org/10.1017/s1047951104001040.
24. Geva T, Ayres NA, Pignatelli RH, Gajarski RJ. Echocardiographic evaluation of common atrioventricular canal defects: a study of 206 consecutive patients. Echocardiography. 1996;13(4):387–400. https://doi.org/10.1111/j.1540-8175.1996.tb00910.x.
25. Laursen HB. Congenital heart disease in Down's syndrome. Br Heart J. 1976;38(1):32–8. https://doi.org/10.1136/hrt.38.1.32.
26. Cetta F, Minich L, Edwards WD, Dearani JA, Puga FJ. Atrioventricular septal defects. In: Allen HD, Driscoll D, Shaddy RE, Feltes TF, editors. Moss and Adams' heart disease in infants, children, and adolescents. 7th ed. Philadelphia, PA: Lippincott Williams & Wilkins; 2008. p. 647–67.
27. Lev M, Liberthson RR, Kirkpatrick JR, Eckner FA, Arcilla RA. Single (primitive) ventricle. Circulation. 1969;39(5):577–91. https://doi.org/10.1161/01.cir.39.5.577.
28. Keane JF, Flyer D. Single ventricle. In: Keane JF, Lock J, Flyer DC, editors. Nadas' pediatric cardiology. 2nd ed. Philadelphia, PA: Saunders Elsevier; 2006. p. 743–51.
29. Fulton DR, Flyer D. D-transposition of the great arteries. Nadas' pediatric cardiology. 2nd ed. Philadelphia, PA: Saunders Elsevier; 2006. p. 645–61.
30. Botto LD, Correa A, Erickson JD. Racial and temporal variations in the prevalence of heart defects. Pediatrics. 2001;107(3):E32. https://doi.org/10.1542/peds.107.3.e32.
31. Blume ED, Altmann K, Mayer JE, Colan SD, Gauvreau K, Geva T. Evolution of risk factors influencing early mortality of the arterial switch operation. J Am Coll Cardiol. 1999;33(6):1702–9. https://doi.org/10.1016/s0735-1097(99)00071-6.
32. Hornung TS, Calder L. Congenitally corrected transposition of the great arteries. Heart. 2010;96(14):1154–61. https://doi.org/10.1136/hrt.2008.150532.
33. Van Praagh R, Van Praagh S. Anatomically corrected transposition of the great arteries. Br Heart J. 1967;29(1):112–9. https://doi.org/10.1136/hrt.29.1.112.
34. Powell AJ, Mandell V. Vascular rings and slings. In: Keane JF, Lock J, Flyer DC, editors. Nadas' pediatric cardiology. 2nd ed. Philadelphia, PA: Saunders Elsevier; 2006. p. 811–23.
35. Kussman BD, Geva T, McGowan FX. Cardiovascular causes of airway compression. Paediatr Anaesth. 2004;14(1):60–74. https://doi.org/10.1046/j.1460-9592.2003.01192.x.
36. Kellenberger CJ. Aortic arch malformations. Pediatr Radiol. 2010;40(6):876–84. https://doi.org/10.1007/s00247-010-1607-9.
37. Edwards JE. Anomalies of the derivatives of the aortic arch system. Med Clin North Am. 1948;32:925–49. https://doi.org/10.1016/s0025-7125(16)35662-0.
38. Dodge-Khatami A, Tulevski II, Hitchcock JF, de Mol BA, Bennink GB. Vascular rings and pulmonary arterial sling: from respiratory collapse to surgical cure, with emphasis on judicious imaging in the hi-tech era. Cardiol Young. 2002;12(2):96–104. https://doi.org/10.1017/s1047951102000239.
39. Edwards JE. Malformations of the aortic arch system manifested as vascular rings. Lab Investig. 1953;2(1):56–75.
40. Fiore AC, Brown JW, Weber TR, Turrentine MW. Surgical treatment of pulmonary artery sling and tracheal stenosis. Ann Thorac Surg. 2005;79(1):38–46. https://doi.org/10.1016/j.athoracsur.2004.06.005; discussion 38–46.
41. Beekman RH. Coarctation of the aorta. In: Allen HD, Driscoll D, Shaddy RE, Feltes TF, editors. Coarctation of the aorta. 7th

ed. Philadelphia, PA: Lippincott Williams & Wilkins; 2008. p. 987–1005.

42. Kocaoglu M, Pednekar AS, Wang H, Alsaied T, Taylor MD, Rattan MS. Breath-hold and free-breathing quantitative assessment of biventricular volume and function using compressed SENSE: a clinical validation in children and young adults. J Cardiovasc Magn Reson. 2020;22(1):54. https://doi.org/10.1186/s12968-020-00642-y.

43. Nguyen KL, Ghosh RM, Griffin LM, Yoshida T, Bedayat A, Rigsby CK, et al. Four-dimensional multiphase steady-state MRI with ferumoxytol enhancement: early multicenter feasibility in pediatric congenital heart disease. Radiology. 2021;300(1):162–73. https://doi.org/10.1148/radiol.2021203696.